

1 Article

2 Using rare earth elements (REE) to study the origin of 3 ore-fluids associated with granite intrusions

4 Xue-Ming Yang

5 Manitoba Geological Survey, 360-1395 Ellice Avenue, Winnipeg, MB R3G 3P2, Canada; eric.yang@gov.mb.ca

6 Received: May 2, 2019; Accepted: date; Published: date

7 **Abstract:** A practical method is presented to estimate rare earth elements (REE) concentrations in
8 magmatic vapour phase (MVP) in equilibrium with water-saturated granitic melts based on
9 empirical fluid-melt partition coefficients of REE (k_p^{REE}). The values of k_p^{REE} can be calculated from a
10 set of new polynomial equations linking to the chlorine molality (m_{Cl}^v) of the MVP associated with
11 granitic melts, which are established via a statistical analysis on the existing experimental dataset.
12 These equations may be applied to the entire pressure range (0.1 to 10.0 kb) within the continental
13 crust, suggesting that light REEs behave differently in magmatic fluids, i.e. either being fluid
14 compatible with higher m_{Cl}^v or fluid incompatible with lower m_{Cl}^v values. In contrast, heavy REEs
15 are exclusively fluid incompatible and partition favourably into granitic melts. Consequently,
16 magmatic fluids tend to be rich in LREE relative to HREE, leading to REE fractionation during the
17 evolution of magmatic hydrothermal systems. Maximum k_p^{REE} value for each element is predicted
18 and presented in a REE distribution diagram constrained by the threshold of m_{Cl}^v . REE contents of
19 the granitic melt is approximated by whole-rock analysis, so that REE concentrations in the
20 associated MVP would be estimated from the value of k_p^{REE} given chemical equilibrium retains.
21 Two examples are provided respectively, to show the use of this method as a REE tracer to
22 fingerprint the source of ore-fluids responsible for the Lake George intrusion-related Au-Sb deposit
23 in New Brunswick (Canada), and for the Bakircay Cu-Au (-Mo) porphyry systems in northern
24 Turkey.

25 **Keywords:** REE distribution pattern; REE fluid-melt partition coefficient; granite; intrusion-related
26 gold system; porphyry copper (gold) system

28 1. Introduction

29 Using rare earth elements (REE) to study the origin of ore-fluids associated with granite (*sensu*
30 *lato*) intrusions has been made possible and attractive, thanks to the progress in a number of high P-T
31 experiments on REE partitioning between magmatic vapour phases and granitic melts [1-3]. This
32 technique has been proved reliable and cost-effective in probing the sources of ore-fluids associated
33 with granite intrusions [4-5].

34 Experimental studies indicate that REE fluid-melt partition coefficient k_p^{REE} (see Table 1 for the
35 explanations of symbols) is dominantly dependent upon fluid composition (i.e. chlorine molality
36 m_{Cl}^v), and is also controlled to some extent by melt composition (e.g., ASI) and pressure (1.25 to 10.0
37 kb), but is not notably affected by temperature (750 to 950 °C) [3]. In a strongly peraluminous (ASI
38 >1.1) granitic melt system associated with a fluid phase with a large range of m_{Cl}^v from 0.1 to 6.0 M,
39 the values of k_p^{La} range from ca. 0.035 to 0.150. In contrast, in a moderately peraluminous (ASI = 1.0
40 to 1.1) to metaluminous (ASI <1.0) melt system associated with fluid phase with the same m_{Cl}^v range,
41 k_p^{La} values range from ca. 0.005 to 1.5 [2-3]. These experimental observations suggest that k_p^{La}
42 values could be estimated over a range of X-P conditions.

43 It is well-known that granitic melts could lose a magmatic vapour phase (MVP; Table 1), shown
44 as trapped fluid inclusions in primary quartz phenocrysts [6-9] to surrounding country rocks during
45 cooling, resulting in hydrothermal alteration and sometimes mineralization (e.g., porphyry Cu-Au
46 (Mo), intrusion-related Au). As much as 5 wt% water containing various metals and/or ligands may

47

Table 1. Symbols used in this paper.

Symbol	Explanation
ASI	Aluminum saturation index that is expressed as molar ratio of Al/(Ca+Na+K) of granitic melts (or granites)
C_{Cl}^m	Chlorine content (wt.%) of granitic melt
C_{REE}^m	REE concentration of granitic melt, e.g., C_{La}^m stands for La content (ppm) in the melt
C_{REE}^v	REE concentration of magmatic fluid (or magmatic vapour phase; see below MVP)
k_p^{Cl}	Chlorine partition coefficient between magmatic fluid and granitic melt, that is defined by the ratio of m_{Cl}^v/m_{Cl}^m
k_p^{REE}	REE partition coefficient between magmatic fluid and granite melt; for example, k_p^{La} denotes La partition coefficient defined by C_{La}^v/C_{La}^m ratio, and so on
m_{Cl}^m	Chlorine molality of granitic melt
m_{Cl}^v	Chlorine molality of magmatic fluid (i.e. aqueous vapour phase)
MVP	Magmatic vapour (or volatile fluid) phase

48

49 be lost to the surroundings upon cooling of granite magmas during their ascent and emplacement
50 [10]. This may be concentrated to form an ore deposit if the geological settings are favourable. The
51 composition of MVP (or magmatic fluids) can be modelled by studying ore-forming elements (e.g.,
52 Cu, Mo) partitioning between the MVP and granitic melts through high PT experimental and
53 empirical investigations [11-13]. Therefore, it is possible to determine what roles are played by the
54 magmatic fluids associated with granitic magmas in mineralization by comparing the geochemical
55 data (e.g., REE) of ore deposits and associated alteration with the composition of simulated
56 magmatic fluids based on the fluid-granitic melt partitioning data.

57 This paper presents the procedures of how to calculate REE concentrations of MVP based on a
58 set of new polynomial equations that can be used for estimation of REE fluid-granitic melt partition
59 coefficients over a wide range of P-T-X conditions. This technique is then used for tracking the
60 sources of ore-fluids responsible for the formation of two typical mineral deposits; 1) the Lake
61 George intrusion-related Sb-Au-W-Mo deposit (New Brunswick, Canada) characterized by low to
62 medium salinity ore-fluids; and 2) the Bakircay Cu-Au (-Mo) porphyry system in northern Turkey,
63 that may have been formed by ore-fluids with medium to high salinities.

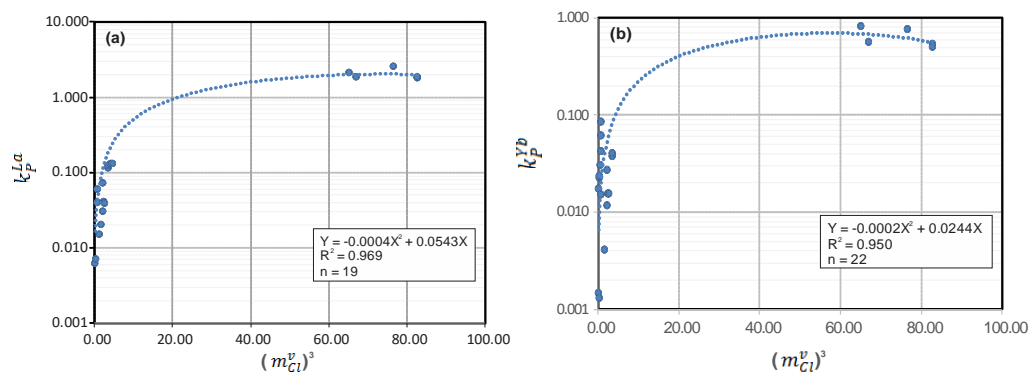
64 2. Methodology

65 An element partition coefficient between MVP and granitic melt is defined by the ratio of its
66 concentration in the MVP to that in the melt [1, 14; Table 1]. For instance, the REE partition
67 coefficient k_p^{REE} between MVP and silicate melt can be expressed as the ratio of C_{REE}^v/C_{REE}^m ; similarly,
68 chlorine partition coefficient k_p^{Cl} is defined as the ratio of m_{Cl}^v/m_{Cl}^m (Table 1). The partition
69 coefficient is dimensionless, and is controlled by various variables, such as pressure, temperature,
70 and composition of magmatic-hydrothermal systems [1-3, 5, 10-16]. It is also noted that the value of
71 k_p^{Eu} could be effected by oxygen fugacity (fO_2) of the system in question, because Eu has two
72 valences (i.e. Eu^{3+} , Eu^{2+}) that depend upon fO_2 [1, 3].

73 Estimates of REE concentration of magmatic fluid are made based on empirical values of k_p^{REE}
74 obtained by the new equations presented in this study (see below); using the REE data of fresh
75 bulk-rock samples to approximate that of the granitic melt in equilibrium with the magmatic fluid,
76 and altered rock, which resulted from the interaction or reaction of the fresh rock with the magmatic
77 fluid. Thus, the signature of magmatic fluids may be recognized to some extent by following the
78 method presented in this study.

79 2.1. Relationship of REE fluid-granitic melt partition coefficient k_p^{REE} to chlorine molality m_{Cl}^v

80 How to calculate REE partition coefficients k_p^{REE} between magmatic aqueous fluid and granite
 81 melt was presented by [5] according to the experimental results [1-2]. It could be described by a
 82 linear function of cubic power of m_{Cl}^v , but the Eu fluid-granitic melt partition coefficient k_p^{Eu} is
 83 related to the fifth power of m_{Cl}^v when the aqueous fluids have relatively low values of m_{Cl}^v . This
 84 confirms the experimental observations by [1-2]. The mathematic relationships of k_p^{REE} to the low
 85 range of m_{Cl}^v of aqueous fluids were provided on the basis of a least square regression analysis of
 86 the experimental dataset. However, such a linear relationship cannot extend to higher values of m_{Cl}^v
 87 (e.g., >3.5 M), which was also noticed by [3]. Therefore, it is necessary to re-assess the existing
 88 experimental data presented in [1-3]. Here, these datasets (Supplementary Table 1) are plotted on
 89 Figure 1, using La to represent LREE and Yb to represent HREE (note: the other REEs are not
 90 shown). To best fit the dataset, a set of new polynomial equations linking k_p^{REE} with m_{Cl}^v can be
 91 obtained for each of REE as shown in Table 2, although more experimental data are required to fill
 92 the data gap. Remarkably, these equations display relatively higher correlation coefficients (R^2
 93 ranging from 0.943 to 0.969; see Table 2) when compared with those (R^2 ranging 0.90 to 0.95)
 94 presented by [5]. Based on the equations presented in Table 2 respectively for La and Yb, k_p^{La} can be
 95 readily calculated, for example, for the magmatic fluid with m_{Cl}^v value of 1.0 M, to be 0.054; and k_p^{Yb}
 96 to be 0.024.
 97



98

99 **Figure 1.** Plot of REE fluid-granitic melt partition coefficient k_p^{REE} versus chlorine molality m_{Cl}^v of
 100 magmatic vapour (fluid) phase: (a) k_p^{La} versus $(m_{Cl}^v)^3$, and (b) k_p^{Yb} versus $(m_{Cl}^v)^3$. Data used for this
 101 plot from [1-3] (Supplementary Table 1). In each of the equation, Y denotes k_p^{REE} ; x represents $(m_{Cl}^v)^3$,
 102 except for Eu where e is $(m_{Cl}^v)^5$ (Table 2); R is correlation coefficient; and n is the number of
 103 experimental dataset. It is worth noting that the uncertainties of such estimation for k_p^{REE} using the
 104 equations listed in Table 2 are not well constrained, although they must have been within the errors
 105 of the original dataset [1-3], i.e. ± 0.025 for LREE, and ± 0.030 for HREE.

106 The REE fluid-granitic melt partition coefficients k_p^{REE} data used for the statistical analysis of
 107 this study (Supplementary Table 1) were acquired under the experimental conditions of 4.0 kb,
 108 800°C and quartz-fayalite-magnetite buffer by [1], at 2.0 kb and 800°C by [2], and experiments at 0.2
 109 to 10 kb and 750 to 950°C by [3]. Numerical analysis of these dataset strongly suggest that k_p^{REE} is
 110 dominantly controlled by chlorine molality m_{Cl}^v of the fluids in equilibrium with the granitic melts,
 111 consistent with the observations by [1-3]. The experiment work indicates that k_p^{REE} values are not
 112 influenced by temperature, although the pressure effect appears to be notable (i.e. the values of k_p^{REE}
 113 for trivalent REEs would increase with decreasing pressure). Interestingly, Borchert et al. (2010) [3]
 114 have pointed out that the pressure (ranging from 2.0 to 9.0 kb) effect on k_p^{La} values is not discernible
 115 for peraluminous granitic melts, although such an effect is slightly manifest for metaluminous melts.
 116 For instance, the value of k_p^{La} increases from 0.03 at 3.0 kb to 0.12 at 7.0 kb when a fluid with m_{Cl}^v of
 117 6.0 M associated with a metaluminous granitic melt [3]. Obviously, more high P-T experiments are
 118 required to cover a range of pressures at least from lower to upper continental crust. Furthermore, it
 119 has been well constrained that k_p^{Cl} is only pressure dependent [10]. Consequently, the value of m_{Cl}^v

120
121
122**Table 2.** Relationship of REE fluid-granite melt partition coefficients (k_p^{REE}) to chlorine molality (m_{Cl}^v) of magmatic fluids [note: x denotes $(m_{Cl}^v)^3$ in the equations except for Eu in which instead of x , a different variable e is used that equals to $(m_{Cl}^v)^5$].

REE	Equation for estimating k_p^{REE}	Correlation coefficient (R^2)	Number of the experimental data used for polynomial analysis (n)
La	$k_p^{La} = -0.0004x^2 + 0.0543x$	0.969	19
Ce	$k_p^{Ce} = -0.0005x^2 + 0.0649x$	0.964	20
Nd	$k_p^{Nd} = -0.0004x^2 + 0.0588x$	0.958	13
Sm	$k_p^{Sm} = -0.0004x^2 + 0.0519x$	0.950	13
Eu	$k_p^{Eu} = -0.0000007e^2 + 0.0017e$	0.956	20
Gd	$k_p^{Gd} = -0.0003x^2 + 0.0419x$	0.943	22
Tb	$k_p^{Tb} = -0.0003x^2 + 0.0413x$	0.956	13
Ho	$k_p^{Ho} = -0.0003x^2 + 0.0338x$	0.965	11
Yb	$k_p^{Yb} = -0.0002x^2 + 0.0244x$	0.950	22
Lu	$k_p^{Lu} = -0.0002x^2 + 0.0207x$	0.962	13

123

124

125

126

127

128

129

130

131

132

133

134

135

136

137

138

139

140

141

in magmatic fluids is only related to pressure (Table 1), which is the main controlling factor on values of k_p^{REE} (Table 2). Therefore, these equations (Table 2) may be used to calculate k_p^{REE} values for a wide range of pressure (0.1 to 10.0 kb) within the continental crust, and to estimate REE concentrations of magmatic fluids, although the limitation of such a practical simulation should be kept in mind.

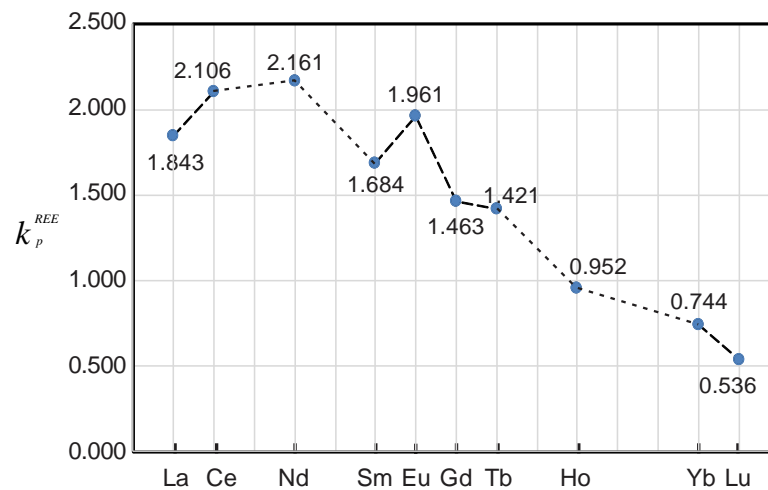
A virtual examination of Figure 1 suggests that the value of k_p^{REE} would approach its maximum with increasing $(m_{Cl}^v)^3$ to a certain value, or a threshold. When $(m_{Cl}^v)^3$ is much smaller than this threshold, k_p^{REE} is in linear relationship to the variable as described by [1-2, 5]. As long as m_{Cl}^v of a magmatic fluid reaches the threshold, the value of k_p^{REE} would reach the maximum and then appear to remain constant regardless how much the concentration of chlorine in the fluid is increased. This conclusion is also achieved by a numerical analysis (i.e. differentiation) of the equations listed in Table 2. This practise is able to predict the $(m_{Cl}^v)^3$ threshold and maximum k_p^{REE} value for each individual element (Table 3). Obviously, the implication of such thresholds and (or) parameters needs further discussed, and tested by more experimental work because the existing dataset used in this paper (Supplementary Table 1) are limited. Albeit the data limitation, the functions presented in Table 2 appear to be applicable to covering the entire pressure range within the continental crust (e.g., 0.1 to 10.0 kb) owing to the fact that maximum k_p^{REE} values rely only upon the chlorine molality thresholds $(m_{Cl}^v)^3$ of magmatic fluids (Figure 2; Table 3) regardless pressures of the

142 fluid-melt systems in question. Here, it is recommended that the maximum value of k_p^{REE} for each
 143 REE be used to simulate REE contents of magmatic fluid once the chlorine molality of the fluid
 144 reaches the threshold.

145 **Table 3.** Predicted chlorine molality thresholds (m_{Cl}^v)³ of magmatic fluids (note: for Eu, it should be
 146 (m_{Cl}^v)⁵) and maximum values of REE fluid-granite melt partition coefficients of k_p^{REE} from this study.

REE	Threshold (m_{Cl}^v) ³ of fluid [except for Eu that is (m_{Cl}^v) ⁵]	m_{Cl}^v of fluid (M)	Maximum value of k_p^{REE}
La	67.88	4.08	1.843
Ce	64.90	4.02	2.106
Nd	73.50	4.19	2.161
Sm	64.88	4.02	1.684
Eu	1214.29	4.14	1.961
Gd	69.83	4.12	1.463
Tb	68.83	4.10	1.421
Ho	56.33	3.83	0.952
Yb	61.00	3.94	0.744
Lu	51.75	3.73	0.536

147



148

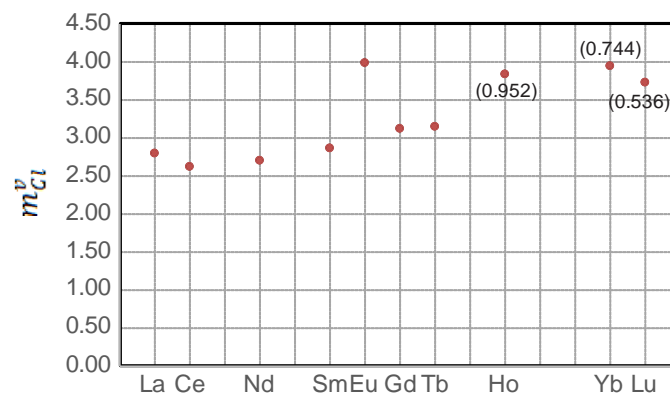
149 **Figure 2.** Plot of the predicted maximum values of REE partition coefficients k_p^{REE} between magmatic
 150 fluids and granitic melts based on the equations in Table 2. Number marked on the graph is the
 151 maximum value of predicted k_p^{REE} for each element, e.g., La equals to 1.843.

152 Figure 2 indicates that REE partitioning between magmatic fluids and granite melts must have
 153 resulted in LREE enrichment relative to HREE in the fluids, consistent with the observations of
 154 alteration halos associated with the Cu-Au (-Mo) porphyry systems [4], intrusion-related Au
 155 systems [5], and of natural fluid inclusions [6]. Also, it is likely that the fluids with relatively low m_{Cl}^v
 156 values would display a negative Eu anomaly as indicated by the relationship of k_p^{REE} to m_{Cl}^v (Table
 157 2), unless their m_{Cl}^v values are close to the threshold that would result in a positive Eu anomaly.
 158 However, this effect could be influenced by the value of m_{Cl}^v that is a function of pressure [10;
 159 14-17]. Maximum partition coefficients for other REE (e.g., Pr, Dy, Er, Tm) may be obtained by
 160 extrapolation from the data presented in Figure 2. Further stretching on this, nevertheless, is not

161 encouraged, although such a practice would provide a basis for future experiment work to
 162 determine their respective values experimentally.

163 Furthermore, the equations (Table 2) can also be used for evaluation of REE behaviour in a
 164 fluid-granitic melt system. When the value of k_p^{REE} is ≥ 1.0 , REE is fluid compatible and prefers
 165 partitioning into the magmatic fluid. Otherwise, REE is granitic melt compatible when k_p^{REE} is < 1.0 .
 166 LREE (e.g., La) would not become fluid compatible until the value of $(m_{Cl}^v)^3$ is higher than 21.97 (i.e.
 167 $m_{Cl}^v \geq 2.80 M$, which is obtained by solving the equation when k_p^{La} equals to 1.0; see Figures 1a and
 168 3). In other words, La would be fluid incompatible and favours granite melt if the fluid has the m_{Cl}^v
 169 value below 2.80 M. Therefore, LREE behaves differently in the fluid-granite melt system,
 170 depending upon the value of m_{Cl}^v of the magmatic fluid. Interestingly, Eu requires much higher m_{Cl}^v
 171 value to become fluid compatible than the other LREE, indicating that it is melt compatible in
 172 equilibrium with magmatic fluids with low m_{Cl}^v , and therefore, such fluids commonly have negative
 173 Eu anomaly. If magmatic fluids reach thresholds $(m_{Cl}^v)^3$ (Table 3; Figure 2), they would display
 174 positive Eu anomaly. HREE (e.g., Yb), however, is typically fluid incompatible and prefers
 175 partitioning into granite melt (Figure 1b), and the maximum value of k_p^{Yb} is 0.744 when $(m_{Cl}^v)^3$ is
 176 equal to its threshold of 61.00 (or $m_{Cl}^v = 3.94 M$) for the fluids associated with granite melts, leading
 177 to REE fractionation that LREE are enriched relatively to HREE during evolution of magmatic
 178 hydrothermal systems.

179 More recently, Song et al. (2016) [18] found that REEs prefer partitioning into carbonate melt
 180 with fluid–melt partition coefficients < 1.0 at 1–2 kb and 700–800 °C, leading to relative HREE
 181 enrichment compared to LREE. Their experimental work suggests that REE fractionation in the
 182 fluid-carbonate melt system distinctly differs from that in the fluid-granite melt system as
 183 discussed in this study.
 184



185
 186 **Figure 3.** Diagram of m_{Cl}^v values required for $k_p^{REE} \geq 1.0$ so that LREEs become fluid compatible,
 187 whereas HREEs are exclusively fluid incompatible and prefer partitioning into granitic melts
 188 because their k_p^{REE} are always < 1.0 and would reach maximum values (as shown by number; Table 3)
 189 when $(m_{Cl}^v)^3$ values achieve their respective threshold.

190 2.2. Calculation of chlorine molality m_{Cl}^v

191 As pointed out by [17], it is not easy to obtain chlorine concentration in granite melt. To make it
 192 simple, the chlorine molality m_{Cl}^m (unit in M or moles/kg) of granitic melt can be calculated by
 193 chlorine content of granite as indicated by the equation below.
 194

$$195 \quad m_{Cl}^m = (C_{Cl}^m \div 35.5) \times [(100 - C_{Cl}^m) \div 1000] \quad (1)$$

196
 197 where chlorine content C_{Cl}^m in granitic melt is approximated by the analysis of whole-rock sample
 198 and its unit is in wt%.

199 Such an exercise of using eq. 1 to calculate chlorine molality m_{Cl}^v of a granite sample would
 200 provide a minimum value of the corresponding granitic melt, because a large amount of chlorine
 201 may have been lost from the melt during cooling [10, 16]. This is unavoidable because of high

202 chlorine partition coefficient between MVP and granitic melt at magmatic conditions [14-15, 17].
 203 Table 4 shows the results of calculation by using two examples.

204 **Table 4.** Calculation of REE concentrations in magmatic fluid.

	Lake Geoge granodiorite [5]		Bakircay granodiorite [4]		
	A	B	D	E	
La (ppm)	30.9	30.9	12.7	12.7	
Ce	51.2	51.2	25.8	25.8	
Nd	13.7	13.7	12.1	12.1	
Sm	4.2	4.2	2.17	2.17	
Eu	1.08	1.08	0.54	0.54	
Gd	4.8	4.8	2.24	2.24	
Tb	0.8	0.8			
Dy			2.25	2.25	
Er			1.16	1.16	
Yb	2.2	2.2	1.1	1.1	
Lu	0.3	0.3			
Cl	1000	15 wt% NaCl _{eqv.} in fluid inclusion [7]	17 wt% NaCl _{eqv.} in primary inclusion	52% NaCl _{eqv.} in fluid inclusion, 18.52 M >Threshold	
<i>Calculation of REE fluid-granitic melt partition coefficient</i>					Equation
m_{Cl}^m	0.028				1
m_{Cl}^v	1.23	3.02	3.50	>Threshold	2
k_p^{Cl}	43.5				at 2 kb [10]
k_p^{La}	0.099	1.189	1.593	1.843	from Table 2
k_p^{Ce}	0.118	1.405	1.863	2.106	from Table 2
k_p^{Nd}	0.107	1.313	1.786	2.161	from Table 2
k_p^{Sm}	0.094	1.123	1.490	1.684	from Table 2
k_p^{Eu}	0.005	0.381	0.700	1.961	from Table 2
k_p^{Gd}	0.076	0.924	1.245	1.463	from Table 2
k_p^{Tb}	0.075	0.908	1.219	1.421	from Table 2
k_p^{Ho}	0.061	0.702	0.898	0.952	from Table 2
k_p^{Yb}	0.044	0.519	0.678	0.744	from Table 2
k_p^{Lu}	0.038	0.418	0.520	0.536	from Table 2
<i>Calculation of REE concentrations (ppm) in MVPs</i>					
C_{La}^v	3.05	36.74	20.23	23.41	
C_{Ce}^v	6.04	71.92	48.08	54.33	
C_{Nd}^v	1.47	17.98	21.61	26.15	
C_{Sm}^v	0.40	4.72	3.23	3.65	
C_{Eu}^v	0.01	0.41	0.38	1.06	
C_{Gd}^v	0.39	4.73	1.43	3.28	
C_{Tb}^v	0.06	0.73			
C_{Yb}^v	0.10	1.14	0.75	2.14	
C_{Lu}^v	0.01	0.14			

205

206 A more accurate chlorine molality m_{Cl}^m of granite melt may be obtained by using the methods
 207 proposed by Piccoli et al. [13], but their methods require chemical composition data of apatite, or
 208 bulk composition of aplite associated with the main granite intrusion. Here, using the value of m_{Cl}^m
 209 obtained by eq. 1 and chlorine partition coefficient k_p^{Cl} [10, 14-15] one can readily estimate the value
 210 of chlorine molality m_{Cl}^v of the aqueous vapour phase in equilibrium with the granite melt at

211 magmatic P-T conditions. As mentioned above, $k_p^{Cl} = m_{Cl}^v/m_{Cl}^m$, is a function of pressure and
 212 independent of temperature within the continental crust [10-11]. Thus, m_{Cl}^v can be obtained from
 213 equation 2 below, if m_{Cl}^m is given (column A in Table 4).

$$214 \quad 215 \quad 216 \quad m_{Cl}^v = k_p^{Cl} \times m_{Cl}^m \quad (2)$$

217 Chlorine partition coefficients k_p^{Cl} between chloride-bearing fluids and granitic melts were
 218 determined experimentally under pressure of 2 to 8 kb and near 700 and 750°C isotherms by Kilinc
 219 and Burnham [14], indicating that the k_p^{Cl} values are strongly dependent upon pressure. The values
 220 increase from 43.5 at 2 kb to 83.3 at 6 kb, and then decrease sharply to 13.0 at 8 kb. Webster and
 221 Holloway (1990) reported a similar result for the pressure range of 2 to 4 kb, although a fluorine-free
 222 system has higher k_p^{Cl} values [15]. These experimental data suggest that chlorine prefers to
 223 partitioning into aqueous fluids under magmatic conditions. However, experiments also showed
 224 that chlorine is compatible to granite melt when it has high fluorine (>7 wt%) and low chlorine (0.12
 225 wt%) contents at 2 kb and 1000°C [15].

226 Using the salinity data of fluid-inclusions to estimate the chlorine molality m_{Cl}^v is a quick
 227 solution regarding the potential problems (e.g., chlorine lost from cooled granitic melts), if the
 228 inclusions trapped in minerals are primary magmatic fluids sourced from granite magmas
 229 (intrusions). For example, the fluid inclusions trapped in apatite enclosed in a plagioclase crystal
 230 from a granodiorite sample collected from the Lake George granodiorite stock represent typical
 231 magmatic fluids with medium salinity of 15 wt% NaCl_{eqv.} that is suitable for calculating chlorine
 232 molality m_{Cl}^v of the fluids [5, 7] (column B in Table 4). This practice may avoid the complexity of
 233 estimating m_{Cl}^m [13, 17] and the use of eq. 2 which relies on the pressure dependant k_p^{Cl} parameter
 234 [14, 15-16].

235 Medium to high salinity fluids (e.g., 17 wt% NaCl_{eqv.}, ~3.50 M Cl⁻; slightly lower salinity than
 236 the threshold required for the maximum value of k_p^{Yb} , see Table 3) are commonly associated with
 237 porphyry Cu-Au (-Mo) systems [19, 20]. These values may be input into the equations to calculate
 238 k_p^{REE} and then to calculate REE concentrations of the magmatic fluids that are presented in column
 239 D in Table 4. High salinity fluids responsible for potassic alteration associated with porphyry Cu-Au
 240 (-Mo) deposits (52 wt% NaCl_{eqv.}, 18.52 M Cl⁻) [20] have much higher values of m_{Cl}^v than the
 241 thresholds (Table 3) required to reach the maximum values of k_p^{REE} for all REE (Table 3; Figure 2).
 242 Thus, using the maximum k_p^{REE} values (Table 3) to calculate REE contents in magmatic fluids is
 243 reasonable, that is presented in column E also in Table 4.

244 2.3. Calculation of REE concentration C_{REE}^v in MVP

245 The REE concentration C_{REE}^v in MVP (magmatic fluids) can be readily calculated in terms of the
 246 k_p^{REE} values as described above and bulk-rock (melt) REE content C_{REE}^m . Table 4 shows that, for
 247 example, La content (3.05 ppm) in the MVP is computed by multiplying the value of k_p^{REE} (0.099)
 248 and La content (30.9 ppm) in the melt that is approxiamted by the analysis of the granite sample
 249 (column A in Table 4).

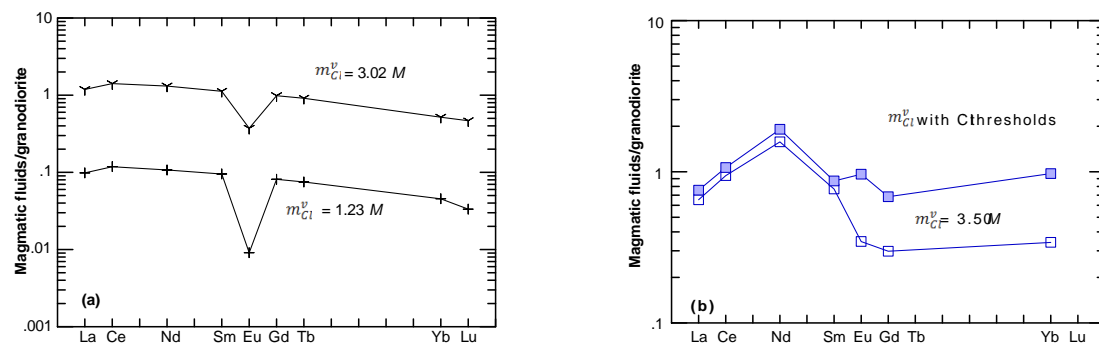
250 3. Application

251 Two examples are presented here to show how to calculate REE concentrations in magmatic
 252 fluid associated with 1) the Lake George granodiorite stock, which is thought to genetically
 253 responsible for the formation of the Sb-Au-W-Mo mineral deposit, New Brunswick (Canada); and 2)
 254 the Bakircay Cu-Au (-Mo) porphyry system, Northern Turkey. The Lake George deposit was the
 255 largest antimony producer in North America until mid-1990s. It is temporally and spatially
 256 associated with the Early Devonian Lake George granodiorite stock [21-27]. The styles of Au
 257 mineralization include Au-bearing quartz-carbonate veins, veinlets and stockworks are present
 258 within the granodiorite stock, quartz-feldspar dyke, and proximal metamorphic aureole; they are
 259 associated with earlier W-Mo mineralization. These characteristics suggest that the Lake George

260 granodiorite intrusion and related hydrothermal systems may have ultimately resulted in Au
 261 mineralization [21-24, 26], resembling intrusion-related gold systems [7, 27-29].

262 Table 4 lists the analyses of the Lake George and Bakircay granodiorites, chlorine contents
 263 either of bulk analysis or from fluid inclusion salinity data, calculated chlorine molality m_{Cl}^v ,
 264 calculated k_p^{REE} and REE concentrations of magmatic fluids. Other data include the Lake George
 265 mineralized quartz-feldspar porphyry [26], Bakircay potassic altered rock [4], and calculated REE
 266 contents in magmatic fluids with different m_{Cl}^v are tabulated in Supplementary Table 2.

267 The Lake George granodiorite-normalized REE distribution patterns of magmatic fluids (see
 268 Table 4 for the estimated value of C_{REE}^v for each element) at chlorine molality m_{Cl}^v equals to 1.23 and
 269 3.02 M, respectively are plotted in Figure 4a, indicating that REE concentrations in the magmatic
 270 fluids are elevated remarkably with increasing the value of m_{Cl}^v (Table 4). Also, the REE pattern of
 271 the fluid displays a pronounced negative Eu anomaly at m_{Cl}^v equal to 1.23 M, whereas the Eu
 272 anomaly becomes much less pronounced when m_{Cl}^v equals to 3.02 M. Figure 4b indicates the REE
 273 patterns in the calculated magmatic fluid at $m_{Cl}^v = 3.50$ M and with thresholds (Table 3), respectively
 274 normalized by the Bakircay granodiorite. Although their LREEs are similar, the fluid with the
 275 threshold Cl⁻ molality displays relatively elevated HREE compared to the granodiorite.
 276

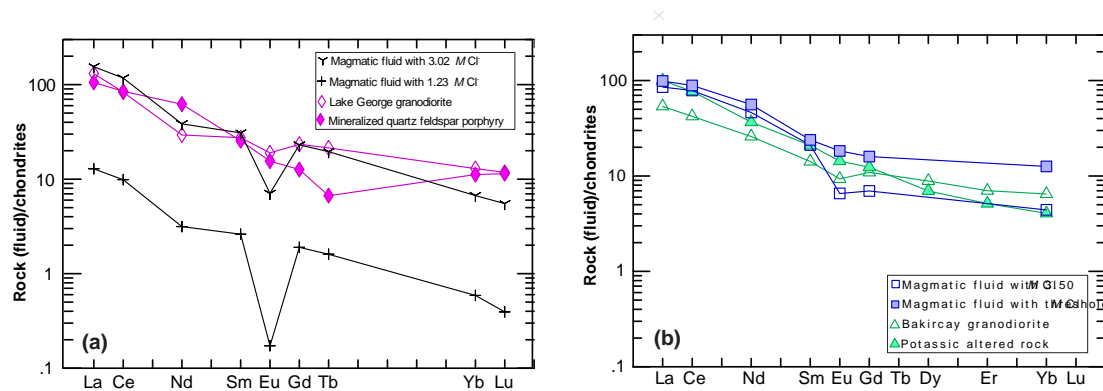


277

278 **Figure 4.** Lake George granodiorite-normalized REE distribution patterns of magmatic fluids with
 279 chlorine molality of m_{Cl}^v equals respectively to 1.23 to M and 3.02 M (a), and the Bakircay
 280 granodiorite-normalized REE distribution patterns of magmatic fluids with m_{Cl}^v values respective of
 281 3.50 M and threshold (b). The normalization values in Table 4.

282 Figure 5a show chondrite-normalized REE patterns for the Lake George granodiorite,
 283 mineralized (or altered) quartz-feldspar porphyry and the calculated magmatic fluids, suggesting
 284 that these fluids are likely to decouple with the granodiorite although the altered porphyry lacks a
 285 Eu anomaly. A higher m_{Cl}^v fluid appears to be required to reduce Eu anomaly, which is evident in
 286 fluid inclusion studies (i.e. halite-bearing inclusions) [7]. Such fluids with varied m_{Cl}^v deriving from
 287 progressively cooling magmas would interact the quartz-feldspar porphyry, resulting in reduction
 288 to disappearance of Eu anomaly, and in some part (HREE) intersecting with the granodiorite. This
 289 process may have produced hydrothermal alteration and simultaneously Au mineralization in the
 290 vein stockwork systems [23, 26], consistent with evidence from litho geochemistry, mineral
 291 chemistry, fluid inclusions, and stable isotopes [7, 27-30]. Notably, increasing the values of m_{Cl}^v
 292 could raise the k_p^{REE} values, thus raises the REE concentration of the ore-fluids, and further reduce
 293 its Eu anomaly.

294 Figure 5b shows the calculated magmatic fluids with m_{Cl}^v of 3.50 M and with threshold
 295 associated with the Bakircay granodiorite melt, and are compared to potassic altered rock that hosts
 296 Cu-Mo mineralization [4], indicating that the mineralization is most likely to related to the ore-fluids
 297 that have medium to very high salinities. Interaction of such fluids with host rocks would have
 298 ultimately resulted in potassic alteration and ore mineral (e.g., chalcopyrite) precipitation. Such
 299 magmatic fluids with LREE enriched relatively to HREE, and released from cooling magmas, are
 300 consistent with the mass-balance studies by [4] and numerical simulation also based on REE
 301 fluid-granitic melt partitioning by [2].
 302



303

304

305

306

307

Figure 5. (a) A comparison of chondrite-normalized REE patterns of calculated magmatic fluids, the Lake George granodiorite and mineralized quartz-feldspar porphyry; (b) chondrite-normalized REE patterns of the Bakircay granodiorite, potassic altered rock, and the calculated magmatic fluids. The chondrite normalizing values are from [31].

308

4. Discussion

309

310

311

312

313

314

315

The experimental data used for this study has not considered chemical components (e.g., CO_3^{2-} , HS-) effect on REE partition coefficients k_p^{REE} except for chlorine concentrations of magmatic fluids [1-3], although the recent experiments show that REEs prefer entering carbonate melt [18], that is a different system. Despite the difficulty of determining chlorine molality (m_{Cl}^v) of granitic melt [17], this study uses the bulk-rock analysis to estimate the minimum value of m_{Cl}^v in the granitic magma (melt), and also suggests that using salinity data of primary fluid inclusions may be a quick solution to this problem (Table 4).

316

317

318

319

320

321

322

323

324

325

326

327

328

The method is presented here to estimate rare earth element concentrations in magmatic fluids associated with water-saturated granites (magmas), which are then compared to those in hydrothermal alteration zones related to intrusion-related Au and porphyry Cu-Au (-Mo) deposits, providing clues as to the origin of their ore-fluids and metallogeny. The key is to estimating the empirical values of k_p^{REE} that have been established and can be described by a set of new polynomial equations (Table 2) based on a statistical analysis of the existing experimental dataset (Supplementary Table 1). These equations (Figure 1 and Table 2) suggest that the values of k_p^{REE} would achieve a maximum when the chlorine molality m_{Cl}^v values are equal to the thresholds (Table 3), which provide a theoretical constraint on REE solubility in magmatic fluids containing chloride. When $m_{Cl}^v >$ thresholds, REE chloride complexes (e.g., LaCl_3 , EuCl_2 , EuCl_3 , YbCl_3) would become unstable at magmatic hydrothermal conditions, and thus some REE minerals (?) may have precipitated. This prediction, however, needs to be tested by experimental work (e.g., using very high salinity solution).

329

330

331

332

333

334

335

336

337

338

339

340

341

342

343

The values of k_p^{REE} in this study are only related to m_{Cl}^v (Table 2) which is linked to k_p^{Cl} that is mainly pressure dependent [14]. Therefore, the equations proposed in this study may be applied to a wide pressure range within the continental crust, given a proper value of k_p^{Cl} at specific pressure [14-16] is used to calculate the value of m_{Cl}^v . As pointed out above, this problem may be readily resolved by using magmatic fluid inclusion data to estimate m_{Cl}^v (Table 4). When the values of m_{Cl}^v reach the thresholds (Table 3), k_p^{REE} would achieve the maximum and therefore must be independent of pressure. Furthermore, LREE and HREE display distinct behaviour in magmatic fluids associated with granitic magmas, leading to their fractionation in the magmatic-hydrothermal systems. The examples given by this study confirm that the calculated magmatic fluids are enriched in LREE relative to HREE (Figure 5), and europium appears to have deviated from the other REEs with either having pronounced negative anomalies (in low to medium m_{Cl}^v fluids) or without notable Eu anomalies (in high m_{Cl}^v fluids). Here, oxygen fugacity is not considered, although it is known that the Lake George granodiorite exhibits characteristics of reduced I-type [27-29] whereas the Bakircay granodiorite is a normal oxidized I-type based on its mineral assemblage [4]. This suggests the behaviour of Eu in the magmatic hydrothermal systems may have been influenced by

344 redox conditions [1]. The Lake George granodiorite contains primary magmatic pyrrhotite, ilmenite
345 but lacks of magnetite, supporting the conclusion that it is a reduced I-type granite [28-30]. The
346 sulphide would be unstable when interacting with chlorine-bearing magmatic fluids, liberating ore
347 components (e.g., Au, S) and enhancing the ore-fluids [28, 32-35] that may have precipitated ore
348 minerals including Au in a suitable setting, e.g., shear zones, hydrofractures, to form
349 intrusion-related gold mineralization [7, 27-28, 36].

350 Although intrusion-related Au systems, such as the Lake George Sb-Au-W-Mo mineral deposit,
351 are commonly characterized by low to medium salinity, carbonic, and reduced ore-fluids [7, 35], the
352 presence of high salinity fluids appears required to balance the LREE, Eu anomaly and HREE as
353 observed in the mineralized porphyry [26] and by the modelling presented in this study. Such a high
354 salinity fluid is evident by the occurrence of halite-bearing fluid inclusions [7, 21-22]. On the other
355 hand, porphyry Cu-Au (-Mo) systems are characterized by oxidized, medium to high salinity (or
356 m_{Cl}^v) ore-fluids [19-20] associated with the granite intrusions. Such conditions are favourable in
357 promoting Cu enrichment during magmatic-hydrothermal evolution [10-14].

358 5. Conclusions

359 LREEs behave differently in magmatic fluids associated with granitic magmas. They are either
360 fluid compatible in higher m_{Cl}^v magmatic fluid or granitic melt compatible in low m_{Cl}^v magmatic
361 fluid, whereas HREE are exclusively fluid incompatible. Consequently, magmatic fluids tend to be
362 rich in LREE relative to HREE, resulting in REE fractionation during the evolution of magmatic
363 hydrothermal systems.

364 When the value of $(m_{Cl}^v)^3$ reaches the threshold, REE fluid-granitic melt partition coefficients
365 k_p^{REE} would achieve their respective maximum value, suggesting that magmatic fluids associated
366 with granitic magmas could not dissolve any more REEs than the predicted maximum
367 concentrations.

368 Europium behaves differently from the other REEs, requiring much higher m_{Cl}^v values to
369 become fluid compatible, and thus the magmatic fluids with low m_{Cl}^v would have a negative Eu
370 anomaly.

371 REE concentrations in magmatic fluids associated with granitic melts (intrusions) may be
372 estimated in terms of the new polynomial equations (Table 2), which are then compared to those of
373 altered and (or) mineralized rocks to study the origin of ore-fluids. This technique is applied to the
374 Lake George Sb-Au-W-Mo mineral deposit, New Brunswick, Canada, and Bakircay Cu-Au (-Mo)
375 porphyry systems in northern Turkey, suggesting that ore-fluids may have been dominated by
376 magmatic fluids, albeit with different chlorine molarities (i.e., the former with low to medium values
377 of m_{Cl}^v , and the latter with medium to high values of m_{Cl}^v).

378 **Supplementary Materials:** The following are available online at www.mdpi.com/xxx/s1, S1: Supplementary
379 Table 1; S2: Supplementary Table 2.

380 **Funding:** This study did not receive any specific grant from funding agencies in the public, commercial, or
381 not-for-profit sectors.

382 **Acknowledgments:** Constructive review of an earlier draft of manuscript by Dr. Sean H. McClenaghan is
383 gratefully acknowledged, which greatly improved the manuscript. Discussion with Simon Gagne is
384 appreciated. I thank two anonymous journal reviewers for their constructive comments on the manuscript,
385 which significantly improved the presentation of this study. The Academic Editor of the journal is gratefully
386 acknowledged for handling the manuscript and for encouraging me to resubmit this paper.

387 **Conflicts of Interest:** The author declares no conflict of interest.

388 References

- 389 1. Flynn, R.; Burnham, C.W. An experimental determination of rare earth partition coefficients between a
390 chlorite containing vapour phase and silicate melts. *Geochimica et Cosmochimica Acta* **1978**, *42*, 685-701.
- 391 2. Reed, M.J.; Candela, P.A.; Piccoli, P.M. The distribution of rare earth elements between monzogranitic

- 392 melt and the aqueous volatile phase in experimental investigations at 800°C and 200 MPa. *Contributions to*
393 *Mineralogy and Petrology* **2000**, *140*, 251-262.
- 394 3. Borchert, M.; Wilke, M.; Schmidt, C.; Cauzid, J.; Tucoulou, R. Partitioning of Ba, La, Yb and Y between
395 haplogranitic melts and aqueous solutions: An experimental study. *Chemical Geology* **2010**, *276*, 225-240.
- 396 4. Taylor, R.P.; Fryer, B.J. Multiple-stage hydrothermal alteration in porphyry copper systems in northern
397 Turkey: The temporal interplay of potassic, propylitic, and phyllic fluids. *Canadian Journal of Earth Sciences*
398 **1980**, *17*, 901-926.
- 399 5. Yang, X.M. Calculation of rare earth element patterns in magmatic fluids: Evidence for origin of the Lake
400 George Sb-Au-W-Mo ore deposit, New Brunswick, Canada. *The Open Geology Journal* **2012**, *6*, 19-24.
- 401 6. Banks, D.A.; Yardley, B.W.D.; Campbell, A.R.; Jarvis, K.E. REE composition of an aqueous magmatic fluid:
402 A fluid inclusion study from the Capitan Pluton, New Mexico, USA. *Chemical Geology* **1994**, *113*, 259-272.
- 403 7. Yang, X.M.; Lentz, D.R.; Chi, G.; Kyser, T.K. Fluid-mineral reaction in the Lake George granodiorite, New
404 Brunswick: implications for Au-W-Mo-Sb mineralization. *Canadian Mineralogist* **2004**, *42*, 1443-1464.
- 405 8. Harlov, D.E.; Austrheim, H. *Metasomatism and the chemical transformation of rock: Rock-mineral-fluid*
406 *interaction in terrestrial and extraterrestrial environments*, 1st ed.; Springer-Verlag: Berlin, Germany 2013; pp.
407 1-16.
- 408 9. Mathieu, L.; Racicot, D. Petrogenetic study of the multiphase Chibougamau Pluton: Archaean magmas
409 associated with Cu-Au magmato-hydrothermal systems. *Minerals* **2019**, *9*, 174; doi:10.3390/min9030174
- 410 10. Holland, H.D. Granites, solutions, and base metal deposits. *Economic Geology* **1972**, *67*, 281-301.
- 411 11. Candela, P.A. Theoretical constraints on the chemistry of the magmatic aqueous phase. In *Ore-bearing*
412 *granite systems; petrogenesis and mineralizing processes*; Stein, H.J., Hannah, J.L., Eds.; Geological Society of
413 America Special Paper 246, 1990; pp. 11-20.
- 414 12. Candela, P.A.; Piccoli, P.M. Magmatic contributions to hydrothermal ore deposits: an algorithm (MVPpart)
415 for calculating the composition of the magmatic volatile phase. *Reviews in Economic Geology* **1998**, *10*,
416 97-108.
- 417 13. Piccoli, P.M.; Candela, P.A.; Williams, T.J. Estimation of aqueous HCl and Cl concentrations in felsic
418 systems. *Lithos* **1999**, *46*, 591-604.
- 419 14. Kilinc, I.A.; Burnham, C.W. Partitioning of chloride between silicate melt and coexisting aqueous phase
420 from 2 to 8 kilobars. *Economic Geology* **1972**, *67*, 231-235.
- 421 15. Webster, J.D.; Holloway, J.R. Partitioning of F and Cl between magmatic hydrothermal fluids and highly
422 evolved granitic magmas. In *Ore-bearing granite systems; petrogenesis and mineralizing processes*; Stein, H.J.,
423 Hannah, J.L., Eds.; Geological Society of America Special Paper 246, 1990; pp. 21-34.
- 424 16. Webster, J.D.; De Vivo, B. Experimental and modeled solubilities of chlorine in aluminosilicate melts,
425 consequences of magma evolution, and implications for exsolution of hydrous chloride melt at Mt.
426 Somma-Vesuvius. *American Mineralogist* **2002**, *87*, 104-1061.
- 427 17. London, D. Estimating abundances of volatile and other mobile components in evolved silicic melts
428 through mineral-melt equilibria. *Journal of Petrology* **1997**, *38*, 1691-1706.
- 429 18. Song, W.L.; Xu, C.; Veksler, I.V.; Kynicky, J. Experimental study of REE, Ba, Sr, Mo and W partitioning
430 between carbonatitic melt and aqueous fluid with implications for rare metal mineralization. *Contributions*
431 *to Mineralogy and Petrology* **2016**, *171*, 1. DOI 10.1007/s00410-015-1217-5
- 432 19. Bodnar, R.J. Fluid inclusion evidence for a magmatic source for metals in porphyry copper deposits.
433 Mineralogical Association of Canada **1995**, *Short Course Series* 23, pp. 139-152.
- 434 20. Gregory, M.J. A fluid inclusion and stable isotope study of the Pebble porphyry copper-gold-molybdenum
435 deposit, Alaska. *Ore Geology Reviews* **2017**, *80*, 1279-1303.
- 436 21. Seal, R.R. II; Clark, A.H.; Morrissy, C.J. Stockwork tungsten (scheelite)-molybdenum mineralization, Lake
437 George, southwestern New Brunswick. *Economic Geology* **1987**, *82*, 1259-1282.
- 438 22. Seal, R.R. II; Clark, A.H.; Morrissy, C.J. Lake George, southwestern New Brunswick: a Silurian,
439 multi-stage, polymetallic (Sb-W-Mo-Au-base metal) hydrothermal centre. In *Recent advances in the geology*
440 *of granite-related mineral deposits*, Taylor, R.P., Strong, D.F., Eds; Canadian Institute of Mining and
441 Metallurgy **1988**, *Special Volume* 39, pp. 252-264.
- 442 23. Lentz, D.R.; Thorne, K.G.; Yang, X.M. Preliminary analysis of the controls on the various episodes of gold
443 mineralization at the Lake George antimony deposit, New Brunswick. In *Current Research, New Brunswick*
444 *Department of Natural Resources and Energy Division 2002, Mineral Resource Report 02-1*, Carroll, B.M.W., Ed.;
445 pp. 55-79.

- 446 24. Yang, X.M.; Lentz, D.R.; Chi, G. Petrochemistry of Lake George granodiorite stock and related gold
447 mineralization, York County, New Brunswick. Geological Survey of Canada, *Current Research* **2002**,
448 *2002-D7*, 1-10.
- 449 25. McLeod, M.J.; Johnson, S.C.; Krogh, T.E. Archived U-Pb (zircon) dates from southern New Brunswick.
450 *Atlantic Geology* **2003**, *39*, 209–225.
- 451 26. Leonard, P.R.R.; Lentz, D.R.; Poujol, M. Petrology, geochemistry, and U-Pb (zircon) age of the
452 quartz-feldspar porphyry dyke at the Lake George antimony mine, New Brunswick: implications for
453 origin, emplacement process, and mineralization. *Atlantic Geology* **2006**, *42*, 13–29.
- 454 27. Yang, X.M.; Lentz, D.R. Sulfur isotopic systematics of granitoids from southwestern New Brunswick,
455 Canada: Implications for magmatic-hydrothermal processes, redox conditions, and gold mineralization.
456 *Mineralium Deposita* **2010**, *45*, 795-816.
- 457 28. Yang, X.M.; Lentz, D.R.; Sylvester, P.J. Gold contents of sulphide minerals in granitoids from
458 southwestern New Brunswick, Canada. *Mineralium Deposita* **2006**, *41*, 369-386.
- 459 29. Yang, X.M.; Lentz, D.R.; Chi, G.; Thorne, K.G. Geochemical characteristics of gold-related granitoids in
460 southwestern New Brunswick, Canada. *Lithos* **2008**, *104*, 355-377.
- 461 30. Yang X.M.; Lentz, D.R. Chemical composition of rock-forming minerals in gold-related granitoid
462 intrusions, southwestern New Brunswick, Canada: Implications for crystallization conditions, volatile
463 exsolution and fluorine–chlorine activity. *Contributions to Mineralogy and Petrology* **2005**, *150*, 287-305.
- 464 31. Sun, S.-s.; McDonough, W.F. Chemical and isotopic systematics of oceanic basalts: implications for mantle
465 composition and processes; In *Magmatism in the Ocean Basins*, Saunders, A.D., Norry, M.J., Eds.; Geological
466 Society of London 1989, Special Publications 42, pp. 313–345.
- 467 32. Keith, J.D.; Whitney, J.A.; Hattori, K.; Ballantyne, G.H.; Christiansen, E.H.; Barr, D.L.; Cannan, T.M.; Hook,
468 C.J. The role of magmatic sulphides and mafic alkaline magmas in the Bingham and Tintic mining
469 districts, Utah. *Journal of Petrology* **1997**, *38*, 1679-1690.
- 470 33. Halter, W.E.; Heinrich, C.A.; Pettke, T. Magma evolution and formation of porphyry Cu–Au ore fluids:
471 Evidence from silicate and sulphide melt inclusions. *Mineralium Deposita* **2005**, *39*, 845-863.
- 472 34. Stavast, W.J.A.; Keith, J.D.; Christiansen, E.H.; Dorais, M.J.; Tingey, D.; Larocque, A.; Evans, N. The fate of
473 magmatic sulfides during intrusion or eruption, Bingham and Tintic Districts, Utah. *Economic Geology*
474 **2006**, *101*, 329-345.
- 475 35. Fan, H.R.; Zhai, M.G.; Xie, Y.H.; Yang, J.H. Ore-forming fluids associated with granite-hosted gold
476 mineralization at the Sanshandao deposit, Jiaodong gold province, China. *Mineralium Deposita* **2003** *38*,
477 739–750.
- 478 36. Yang, X.M. Sulphur solubility in felsic magmas: implications for genesis of intrusion-related gold
479 mineralization. *Geoscience Canada* **2012**, *39*, 17-32.